

Published in final edited form as:

Eur J Neurosci. 2005 September ; 22(5): 1257–1262. doi:10.1111/j.1460-9568.2005.04304.x.

Synapse Independence Breaks Down During Highly Synchronous Network Activity in the Rat Hippocampus

Ágota A. Biró and Zoltan Nusser

Laboratory of Cellular Neurophysiology, Institute of Experimental Medicine, Hungarian Academy of Sciences, Szigyony Street 43, 1083 Budapest, Hungary

Abstract

The discharge pattern of hippocampal pyramidal cells (PC) varies depending on the behaviour of the animal and on the accompanying network states. During theta activity, PCs fire asynchronously at low rates whereas during sharp waves PCs increase their firing frequency and many cells fire synchronously. In the present study, we addressed how the presynaptic activity of CA1 PCs influences the precise operation of their output synapses. Asynchronous presynaptic discharge was mimicked by activating only a single PC during paired recordings, whereas the highly synchronous presynaptic firing was emulated by extracellularly stimulating the axons of ≈ 70 PCs in acute hippocampal slices. By using low- and high-affinity glutamate receptor competitive antagonists to monitor the synaptic glutamate concentration transient, we show that the synaptic transmitter concentration varies depending on the release probability (P_r) when many

Correspondence: Dr Zoltan Nusser, as above. E-mail: nusser@koki.hu.

Abbreviations

AP action potential

CNQX 6-cyano-2,3-dihydroxy-7-nitro-quinoxaline

eEPSC evoked EPSC

EPSC excitatory postsynaptic current

cDGG c-D-glutamyl-glycine

mGluR metabotropic glutamate receptor

O-Bi oriens-bistratified

O-LM oriens-lacunosum moleculare

PC hippocampal pyramidal cell

P_r release probability

q quantal size

R_s series resistance

τ_w weighted decay time

uEPSC unitary EPSC.

fibres are synchronously activated. Our kinetic analysis revealed that an 5-fold increase in P_T from the beginning to the end of an action potential train resulted in a slowing down of the decay of \approx evoked EPSCs, suggesting neurotransmitter spillover between neighbouring synapses. In agreement with this prediction, the slowing of the decay was reversed by the application of the low-affinity antagonist γ -D-glutamyl-glycine. In contrast, altering P_T had no effect on the kinetics of unitary EPSCs. Our data demonstrate that synapse independence breaks down during synchronous presynaptic activity, but the point-to-point communication is preserved when PCs fire asynchronously.

Keywords

interneurons; paired recordings; spillover

Introduction

The exquisitely precise anatomical arrangement between pre- and postsynaptic specializations of chemical synapses prompted the view of a specific, point-to-point signalling between central neurons. In agreement with this morphological prediction, synapse independence was among the basic assumptions of the classical quantal theory (del Castillo & Katz, 1954). Namely, it was assumed that release sites operate independently and at each release site either zero or only one vesicle is released. As a consequence, the size of the postsynaptic response (q , quantal size) at a given release site is not influenced by the activity of its neighbouring synapses.

However, this view of synaptic function is clearly an over-simplification. Several recent studies have revealed that more than one vesicle might be released from one release site (multivesicular release) within a very short period of time (< 1 ms) following the arrival of a single action potential (AP; Tong & Jahr, 1994; Auger *et al.*, 1998; Wadiche & Jahr, 2001; Oertner *et al.*, 2002). When multivesicular release occurs at a single release site q will depend on the release probability (P_T), but the specificity or point-to-point operation of synapses will prevail. However, if transmitter released at a given release site affects q or P_T at the neighbouring release sites following its intersynaptic diffusion (a phenomenon called spillover or cross-talk), the point-to-point nature of communication will no longer characterize the connection. This is not just a theoretical possibility, because intersynaptic spillover has been convincingly demonstrated at a number of glutamatergic and GABAergic synapses (reviewed by Barbour & Hausser, 1997; Kullmann & Asztely, 1998; Isaacson, 2000; Jahr, 2003). Examples of glutamate spillover include the activation of high-affinity metabotropic glutamate receptors (mGluRs) on neighbouring glutamatergic and GABAergic axon terminals (Scanziani *et al.*, 1997; Mitchell & Silver, 2000; Semyanov & Kullmann, 2000) and high-affinity NMDA receptors located either extrasynaptically or in neighbouring synapses (Asztely *et al.*, 1997; Isaacson, 1999; Carter & Regehr, 2000; Diamond, 2001; Clark & Cull-Candy, 2002; Scimemi *et al.*, 2004). Much less is known about whether AMPA receptors could also be activated in a similar manner. AMPA receptors have a lower affinity for glutamate and desensitize very rapidly and extensively, rendering them insensitive for activation by low-amplitude, slow glutamate transients (Asztely *et al.*, 1997). Despite this, a few studies have reported the spillover-mediated activation of AMPA receptors (Carter & Regehr, 2000; DiGregorio *et al.*, 2002). In our recent study (Biro *et al.*, 2005), we have demonstrated that when only a single presynaptic hippocampal pyramidal cell (PC) is activated its output synapses operate independently; no sign of multivesicular release or spillover was observed. However, PCs do not always fire on their own at low frequency, because their activity varies depending on the behaviour of the animal and on the accompanying network state. During hippocampal theta activity CA1 PCs show

asynchronous activity and fire at a very low frequency. In contrast, during sharp waves PCs increase their firing frequency > 100-fold and many cells fire synchronously (reviewed by Buzsáki, 2002). In the present study, we asked how the presynaptic activity of CA1 PCs influences the precise operation their output synapses.

Materials and methods

Slice preparation and electrophysiological recordings

Acute hippocampal slices were prepared from 14- to 18-day-old male Wistar rats, under ketamine anaesthesia (50 mg per animal), as described earlier (Biro *et al.*, 2005). Briefly, horizontal slices were cut with a Vibratome and were stored in a continuously oxygenated ACSF at 30 °C. Slices transferred to the recording chamber were perfused with an ACSF containing (in mM) NaCl, 126; KCl, 2.5; glucose, 25; NaH₂PO₄, 1.25; NaHCO₃, 24; MgCl₂, 2; and CaCl₂, 2, and a GABA_A receptor antagonist (20 μM SR95531). Recordings were performed at 32-36 °C. During paired recordings, presynaptic CA1 PCs were recorded in a whole-cell current-clamp configuration using a K-gluconate-based intracellular solution (in mM: K-gluconate, 120; KCl, 5; MgCl₂, 2; EGTA, 0.05; HEPES, 10; Na-ATP, 2; Na-GTP, 0.4; creatinine phosphate, 10; L-glutamic acid, 10; and biocytin, 5.3) of pH 7.25 and osmolarity 270-290 mOsm. Trains of action potentials (at 50 Hz) were evoked at 0.03-0.06 Hz by injecting 10-40 short (3 ms) depolarizing currents. Unitary excitatory postsynaptic currents (uEPSCs) were recorded in the postsynaptic stratum interneurons located in stria oriens or alveus, voltage-clamped at -70 mV (pipette solution as for the presynaptic cells without L-glutamic acid but with 130 mM K-gluconate; pH 7.25, osmolarity 270-290 mOsm). For simultaneous stimulation of several presynaptic fibres, EPSCs were evoked by extracellular stimulation (6 or 10 stimuli at 50 Hz in every 15 s) with a theta-glass pipette placed in the stratum oriens. Oriens-lacunosum moleculare (O-LM) and some oriens-bistratified (O-Bi) interneurons were successfully preselected according to their differential interference contrast image, somatic location and their firing patterns (see Losonczy *et al.*, 2002; Biro *et al.*, 2005). Recordings were performed with a dual-channel amplifier (Multiclamp 700 A, Molecular Devices Inc., Union City, CA, USA), filtered at 3 or 4 kHz (Bessel filter), digitized at 20 kHz and analysed with in-house-written software (EVAN3.1). Series resistance (R_s) and whole-cell capacitance was checked every 2 min in the interneurons. The mean R_s was 15.5 ± 0.6 MΩ and after 60-85% compensation it was 4.1 ± 0.2 MΩ ($n = 34$). Significance of differences was evaluated with *t*-tests. Data are given as mean \pm SEM. All chemicals and drugs were purchased from Sigma with the exception of γ -D-glutamyl-glycine (γ DGG) and CNQX (6-cyano-2,3-dihydroxy-7-nitro-quinoxaline, Tocris Cookson, Bristol, UK).

Data analysis

To ensure the time-independence of our data during the recordings, we used the following criteria. The compensated R_s was measured every 2 min. If the slope of a regression line fitted to the scatter plot of R_s vs. time significantly differed from zero ($P < 0.01$, *t*-test), the recording was discarded. For pharmacological experiments, if the R_s changed > 15% from the control to the drug period, the recording was also discarded. All recordings were rejected when the R_s became > 25 MΩ. For all pharmacological experiments, a control period of 5 min before the start of the drug application was compared to time windows with the same length after 10 min of wash-in of the drug. We considered different segments of stimulus trains as different P_r conditions (see Biro *et al.*, 2005). All recordings where the 10-90% rise time of EPSCs exceeded 1.0 ms were also rejected. For the kinetic analysis, a minimum of 40 trains of uEPSCs were required to include a pair in our study. We measured the failure rate, the amplitude and 10-90% rise time at the beginning and end of the stimulus trains for both unitary and evoked EPSCs. The weighted decay time (τ_w) was calculated from

exponential fits as $\tau_w = \tau_1 * A_1 + \tau_2 * (1 - A_1)$, where τ_1 and τ_2 are the fast and slow decay time constants, respectively, and A_1 is the contribution of the first exponential to the amplitude.

Results

In the present study, whole-cell voltage-clamp recordings were carried out from interneurons located in stratum oriens or alveus in acute hippocampal slices of juvenile rats at 34 °C to address how the fine operation of hippocampal glutamatergic synapses is influenced by different presynaptic activity patterns. Asynchronous presynaptic activity was mimicked by activating only a single CA1 PC during paired recordings, whereas extracellular stimulation of several CA1 PC axons was carried out to approximate highly synchronous presynaptic firing. During paired recordings, short trains of presynaptic APs at 50 Hz evoked facilitating ($5.0 \pm 0.7 \times$ facilitation, $n = 10$) uEPSCs in O-LM and in some O-Bi cells. Extracellular stimulation-evoked EPSCs (eEPSCs) in O-LM and O-Bi interneurons showed a very similar short-term plasticity pattern with an average of $4.8 \pm 1.0 \times$ ($n = 16$) facilitation from the beginning to the end of the stimulus train (Fig. 1A and B). Extracellular stimulation experiments and paired recordings were performed on different populations of the same interneuron types. Because eEPSCs (57.0 ± 7.2 pA, $n = 16$) had on average $5.7 \times$ larger amplitudes than uEPSCs (10.1 ± 2.3 pA, $n = 10$) at the beginning of the stimulus trains, and because only every 12th PC was coupled to an O-LM or O-Bi cell in our slice preparation (Biro *et al.*, 2005), we estimated that our extracellular stimulation activated on average ≈ 70 PCs, six of which were making direct synapses (on average three synapses per connection) on our recorded interneuron.

We have previously demonstrated that short-term facilitation of unitary EPSCs evoked in O-LM or O-Bi cells by CA1 PCs was the sole consequence of an increase in P_r with no alterations in quantal amplitudes, indicating a lack of multivesicular release or intersynaptic spillover (Biro *et al.*, 2005). First, we asked whether an increased P_r could also fully account for the short-term facilitation when many presynaptic fibres were synchronously activated. In our previous study, the morphological identification of the activated synapses was essential for constraining the number of parameters in our quantal analysis. However, it is impossible to utilize this approach when the presynaptic fibres are extracellularly stimulated. To circumvent this technical difficulty, we employed pharmacological tools (Clements *et al.*, 1992) to estimate the glutamate concentration transient underlying eEPSCs. If multivesicular release and transmitter spillover does not take place at these synapses, the spatio-temporal profile of the glutamate concentration should be identical at low-(beginning) and high-(end of the stimulus train) P_r conditions. Thus, a low-affinity competitive antagonist is expected to block eEPSCs to a similar extent throughout the stimulus train. However, in the presence of multivesicular release or intersynaptic spillover, the glutamate concentration transient is expected to be higher and slower at high P_r , resulting in a smaller degree of block by a low-affinity antagonist (Clements *et al.*, 1992; Wadiche & Jahr, 2001; DiGregorio *et al.*, 2002). We tested this hypothesis by using the low-affinity competitive non-NMDA receptor antagonist γ DGG. The application of 0.5 mM γ DGG resulted in a significantly smaller block of the peak amplitude of eEPSCs under high- than low- P_r conditions (52 ± 3 vs. $63 \pm 3\%$, $n = 11$, $P < 0.05$, t-test; Fig. 1A and C). This distinction was not observed when a slowly dissociating high-affinity antagonist CNQX (1 μ M) was applied under identical conditions (beginning, $64 \pm 4\%$; end, $65 \pm 3\%$, $n = 12$; Fig. 1B and C). As a consequence, an enhanced short-term facilitation was observed in the presence of γ DGG (from 5.1 ± 0.9 to $7.3 \pm 1.6 \times$, $n = 11$), but not in CNQX (4.9 ± 0.8 and $4.5 \pm 0.6 \times$, $n = 12$; Fig. 1D). These differential inhibitions of eEPSCs by low- and high-affinity antagonists indicate that the effect of γ DGG is likely to be due to a P_r -dependent alteration in the synaptic glutamate concentration transient instead of a potential presynaptic drug effect on the transmitter release.

If intersynaptic transmitter spillover was indeed responsible for the increase in the cleft transmitter concentration at high P_r conditions, a slowing of the decay time constant would also be expected during the stimulus train. This is because the increase in P_r can be considered an increase in the density of active boutons around the recorded postsynaptic cell's somato-dendritic domain, from which more and more transmitter can reach and activate AMPA receptors (DiGregorio *et al.*, 2002). To test this prediction, we have performed kinetic analysis of the eEPSCs. The weighted decay time constant of eEPSCs was significantly slower ($P < 0.01$, *t*-test) at the end of the stimulus train than at the beginning (beginning, 2.6 ± 0.2 ms; end, 3.7 ± 0.4 ms, $n = 16$; Fig. 2D-F). When the ratio of decay time constants at the end and at the beginning of the train was calculated in each cell, approximately one-quarter of the cells had a ratio close to one, whereas three-quarters of the cells showed significant slowing of the decay (Fig. 2E). If a slower and lower glutamate concentration transient is responsible for the late, slow phase of the eEPSC decay, the low-affinity antagonist γ DGG should preferentially block the slow, spillover component and therefore speed up the decay. Indeed, the application of 0.5 mM γ DGG accelerated the decay of the eEPSCs. At high P_r , γ DGG resulted in a $31 \pm 8\%$ speeding of the decay (from 3.6 ± 0.4 to 2.3 ± 0.2 ms, $n = 9$) whereas at low P_r the acceleration of the decay was somewhat smaller ($26 \pm 10\%$, from 2.4 ± 0.3 to 1.7 ± 0.3 ms, $n = 9$), but was still significant (Fig. 3). As a control, we also repeated the same experiments with the high-affinity antagonists CNQX and found no effect on the decay of eEPSCs (Fig. 3), consistent with the slow dissociation of CNQX from the receptors compared to the glutamate transient. Neither at the beginning (from 2.7 ± 0.5 to 2.2 ± 0.3 ms, $n = 6$) nor at the end of the stimulus train (from 4.0 ± 0.9 to 3.9 ± 1.0 ms, $n = 6$) had CNQX changed the decay of eEPSCs. Our kinetic analysis taken together with the effect of the low-affinity antagonists indicate that the glutamate concentration profile underlying evoked EPSCs is influenced by the transmitter release probability. Our previous work (Biro *et al.*, 2005) predicted the lack of such an effect when only a single presynaptic PC was activated. This would also forecast that the kinetics of the uEPSC is constant during the stimulus train. Indeed, as shown in a representative cell in Fig. 2, the pronounced facilitation during the train had no effect on the decay times of unitary EPSCs at low ($\tau_w = 0.73$ ms) and high ($\tau_w = 0.82$ ms) P_r conditions. When we calculated the ratio of decay times at the end and at the beginning of the train in every cell, the values clustered around unity with a mean of 1.02 ± 0.04 ($n = 11$; Fig. 2B), demonstrating that the P_r -independence of uEPSC kinetics is also true for the whole population.

Discussion

The results of our kinetic analysis revealed a robust slowing of the decay of eEPSCs during the stimulus train, whereas that of the uEPSCs was not affected by alterations in P_r . The slowing of the eEPSC decay could be reversed by a low-but not a high-affinity non-NMDA receptor antagonist, indicating that the synaptic glutamate concentration transient underlying the eEPSCs varies depending on P_r . In agreement with this, a differential block of evoked EPSC amplitudes by γ DGG was also observed during the stimulus trains. Because the quantal amplitude and the kinetics of unitary EPSCs are independent of P_r , and because the only difference between the unitary and extracellularly evoked responses was the number of simultaneously stimulated fibres we concluded that, when a large number of presynaptic PCs are simultaneously active, intersynaptic spillover of glutamate influences the postsynaptic responses at neighbouring synapses.

As pointed out by Jahr (2003) in a recent review, distinguishing between multivesicular release and intersynaptic spillover as the mechanism underlying altered transmitter concentration transients is almost impossible with the currently available physiological and pharmacological techniques. Thus, the results of our kinetic analysis and pharmacological

experiments are consistent with both of these mechanisms being responsible for the P_r -dependent increase in the glutamate concentration transient. The reason why we believe that it is more likely that intersynaptic spillover underlies the alteration is as follows. If multivesicular release took place at these synapses, one would expect multivesicular release to occur when only a single presynaptic input is activated. This is inconsistent with the kinetic analysis of uEPSCs in the present study and also with the results of combined physiological and morphological experiments of our previous work (Biro *et al.*, 2005). From the amplitude of evoked and unitary responses at the beginning of the stimulus train and from the connectivity probability between CA1 PCs and O-LM or O-Bi interneurons in our slice preparations, we estimated that ≈ 70 PC axons were stimulated by our extracellular electrode, six of which made direct synapses on the recorded interneuron. Thus, the major difference between evoked and unitary EPSCs is that for the former $\approx 70\times$ more presynaptic fibres are activated, resulting in a 70-fold increase in the active bouton density in the hippocampal neuropile. The exact number of axon terminals of a CA1 PC in the space occupied by the somato-dendritic domains of O-LM cells is unknown, but we estimated it to be several hundreds, resulting in potentially over 10 000 axon terminals that may release transmitter.

Although we have used a short high-frequency train to activate the presynaptic fibres, our results clearly demonstrate that high-frequency stimulations were not necessary for spillover to occur. As expected, a larger degree of spillover is observed at the end of the stimulus train than at the beginning, but γ DGG had already significantly speeded up the decay of eEPSCs at the beginning of the train. However, during hippocampal sharp waves when CA1 PCs fire in synchrony they also fire more than one AP at high frequency so our stimulation protocol may also be representative for the activity during this hippocampal network state. Other experiments showing spillover-mediated AMPA receptor activation concluded that either high-frequency stimulation was required (Carter & Regehr, 2000) or a single stimulus was already sufficient (DiGregorio *et al.*, 2002; Nielsen *et al.*, 2004), depending on the type of synaptic connection. Our results demonstrate that when multiple fibres are activated simultaneously in a cortical region, a single presynaptic stimulus is sufficient to induce significant AMPA receptor-mediated spillover between neighbouring synapses, the degree of which is increased upon repetitive activation.

Whether glutamatergic synapses operate independently or intersynaptic crosstalk occurs has profound consequences on neuronal network functions such as its information storage capacity (Abbott & Regehr, 2004). One of the most important findings of our results is that the computational power of the network is not constant, but depends on the behaviour of the animal and on the accompanying network state. It is well known that CA1 PCs show asynchronous activity and fire at a very low frequency during hippocampal theta activity, a prominent network activity associated with exploration, memory tasks and rapid-eye-movement sleep. In contrast, during sharp waves, a hippocampal state that is implicated in memory consolidation and occurs during slow-wave sleep and consummatory behaviours, PCs increase their firing frequency > 100 -fold and many cells fire synchronously (Csicsvari *et al.*, 1998). As discussed above, during extracellular stimulation, we have activated ≈ 70 PCs that comprise ≈ 0.1 - 0.2% of all CA1 PCs that could potentially make synapses on our recorded interneuron. This number is still 5-10 times lower than the proportion of CA1 PCs that exhibit synchronous activity during sharp waves within a time window of 1 ms (J. Csicsvari, personal communication). Thus, the degree of intersynaptic spillover is expected to be even more pronounced during hippocampal sharp waves than what we have observed in our experiments. It is needless to say that one should be cautious when making predictions about the operation of synapses in behaving animals from the results of *in vitro* experiments. However, until similar experiments can be performed *in vivo* in behaving

animals, the predictions of *in vitro* experiments may be taken into account when the operation of synapses is approximated in network models.

Acknowledgments

Z.N. is the recipient of a Wellcome Trust International Senior Research Fellowship, an International Scholarship from Howard Hughes Medical Institute and a Postdoctoral Fellowship from the Boehringer Ingelheim Fond. The financial support from these Foundations is greatly acknowledged. We would like to thank Drs Mark Eyre, Mark Farrant and Istvan Mody for their comments on the manuscript.

References

- Abbott LF, Regehr WG. Synaptic computation. *Nature*. 2004; 431:796–803. [PubMed: 15483601]
- Asztely F, Erdemli G, Kullmann DM. Extrasynaptic glutamate spillover in the hippocampus: dependence on temperature and the role of active glutamate uptake. *Neuron*. 1997; 18:281–293. [PubMed: 9052798]
- Auger C, Kondo S, Marty A. Multivesicular release at single functional synaptic sites in cerebellar stellate and basket cells. *J. Neurosci*. 1998; 18:4532–4547. [PubMed: 9614230]
- Barbour B, Hausser M. Intersynaptic diffusion of neurotransmitter. *Trends Neurosci*. 1997; 20:377–384. [PubMed: 9292962]
- Biro AA, Holderith NB, Nusser Z. Quantal size is independent of the release probability at hippocampal excitatory synapses. *J. Neurosci*. 2005; 25:223–232. [PubMed: 15634785]
- Buzsaki G. Theta oscillations in the hippocampus. *Neuron*. 2002; 33:325–340. [PubMed: 11832222]
- Carter AG, Regehr WG. Prolonged synaptic currents and glutamate spillover at the parallel fiber to stellate cell synapse. *J. Neurosci*. 2000; 20:4423–4434. [PubMed: 10844011]
- del Castillo J, Katz B. Statistical factors involved in neuromuscular facilitation and depression. *J. Physiol. (Lond.)*. 1954; 124:574–585. [PubMed: 13175200]
- Clark BA, Cull-Candy SG. Activity-dependent recruitment of extrasynaptic NMDA receptor activation at an AMPA receptor-only synapse. *J. Neurosci*. 2002; 22:4428–4436. [PubMed: 12040050]
- Clements JD, Lester RA, Tong G, Jahr CE, Westbrook GL. The time course of glutamate in the synaptic cleft. *Science*. 1992; 258:1498–1501. [PubMed: 1359647]
- Csicsvari J, Hirase H, Czurko A, Buzsaki G. Reliability and state dependence of pyramidal cell-interneuron synapses in the hippocampus: an ensemble approach in the behaving rat. *Neuron*. 1998; 21:179–189. [PubMed: 9697862]
- Diamond JS. Neuronal glutamate transporters limit activation of NMDA receptors by neurotransmitter spillover on CA1 pyramidal cells. *J. Neurosci*. 2001; 21:8328–8338. [PubMed: 11606620]
- DiGregorio DA, Nusser Z, Silver RA. Spillover of glutamate onto synaptic AMPA receptors enhances fast transmission at a cerebellar synapse. *Neuron*. 2002; 35:521–533. [PubMed: 12165473]
- Isaacson JS. Glutamate spillover mediates excitatory transmission in the rat olfactory bulb. *Neuron*. 1999; 23:377–384. [PubMed: 10399942]
- Isaacson JS. Spillover in the spotlight. *Curr. Biol*. 2000; 10:R475–R477. [PubMed: 10898970]
- Jahr CE. Drooling and stuttering, or do synapses whisper. *Trends Neurosci*. 2003; 26:7–9. [PubMed: 12495854]
- Kullmann DM, Asztely F. Extrasynaptic glutamate spillover in the hippocampus: evidence and implications. *Trends Neurosci*. 1998; 21:8–14. [PubMed: 9464678]
- Losonczy A, Zhang L, Shigemoto R, Somogyi P, Nusser Z. Cell type dependence and variability in the short-term plasticity of EPSCs in identified mouse hippocampal interneurons. *J. Physiol. (Lond.)*. 2002; 542:193–210. [PubMed: 12096061]
- Mitchell SJ, Silver RA. Glutamate spillover suppresses inhibition by activating presynaptic mGluRs. *Nature*. 2000; 404:498–502. [PubMed: 10761918]
- Nielsen TA, DiGregorio DA, Silver RA. Modulation of glutamate mobility reveals the mechanism underlying slow-rising AMPAR EPSCs and the diffusion coefficient in the synaptic cleft. *Neuron*. 2004; 42:757–771. [PubMed: 15182716]

- Oertner TG, Sabatini BL, Nimchinsky EA, Svoboda K. Facilitation at single synapses probed with optical quantal analysis. *Nat. Neurosci.* 2002; 5:657–964. [PubMed: 12055631]
- Scanziani M, Salin PA, Vogt KE, Malenka RC, Nicoll RA. Use-dependent increases in glutamate concentration activate presynaptic metabotropic glutamate receptors. *Nature.* 1997; 385:630–634. [PubMed: 9024660]
- Scimemi A, Fine A, Kullmann DM, Rusakov DA. NR2B-containing receptors mediate cross talk among hippocampal synapses. *J. Neurosci.* 2004; 24:4767–4777. [PubMed: 15152037]
- Semyanov A, Kullmann DM. Modulation of GABAergic signaling among interneurons by metabotropic glutamate receptors. *Neuron.* 2000; 25:663–672. [PubMed: 10774733]
- Tong G, Jahr CE. Multivesicular release from excitatory synapses of cultured hippocampal neurons. *Neuron.* 1994; 12:51–59. [PubMed: 7507341]
- Wadiche JI, Jahr CE. Multivesicular release at climbing fiber-Purkinje cell synapses. *Neuron.* 2001; 32:301–313. [PubMed: 11683999]

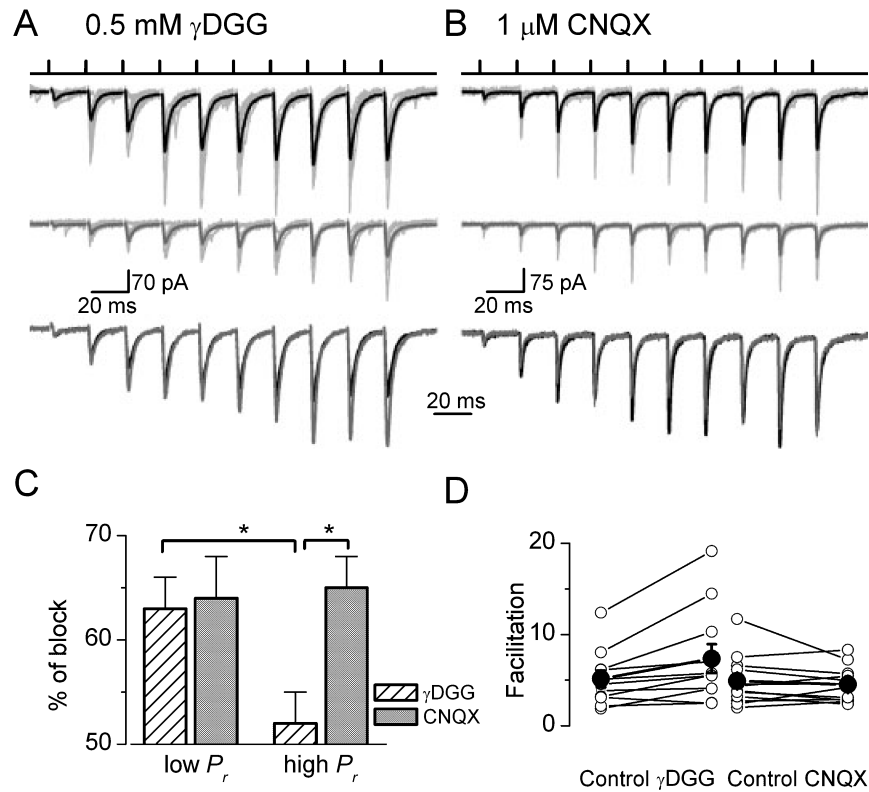


Fig. 1. Differential block of evoked EPSC amplitudes by (A) low- and (B) high-affinity competitive antagonists. Short trains of extracellular stimuli (top traces) evoke facilitating EPSCs in interneurons located in stata oriens or alveus. A, cell AB517; B, cell AB528. Averaged EPSCs are shown in control (thick black traces) and in the presence of (A) γ DGG and (B) CNQX (thick grey traces). Individual traces are thin light grey. The averaged EPSCs scaled to the peak of the first events are superimposed in control and after the application of (A, bottom panel) γ DGG and (B, bottom panel) CNQX. (A) An enhanced facilitation is seen in the presence of γ DGG, but (B) the short-term dynamism is the same in the CNQX as in control. (C) The application of γ DGG resulted in a significantly ($P < 0.05$) smaller inhibition of evoked EPSC amplitudes under high- than under low- P_r conditions. The high-affinity antagonist CNQX caused a similar amount of block at both P_r conditions. (D) The degree of facilitation of EPSCs from the beginning to the end of the stimulus train is plotted in control conditions and in the presence of glutamate receptor antagonists (O, individual cells; •, means \pm SEM). The facilitation increased significantly following the application of γ DGG, but remained practically unchanged after the application of CNQX.

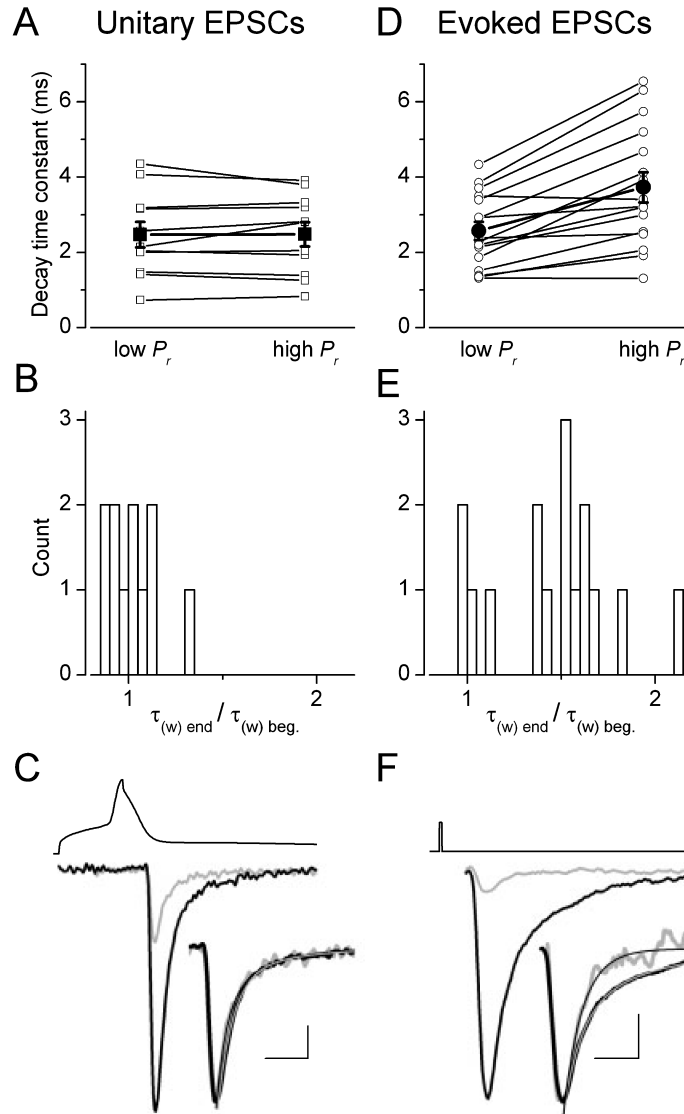


Fig. 2. Analysis of decay kinetics of unitary and extracellularly evoked EPSCs. (A and D) The decay time constant of unitary EPSCs remained constant whereas that of extracellular stimulation-evoked EPSCs was slower at the end of the stimulus trains than at the beginning (open symbols, individual pairs; filled large symbols, mean \pm SEM). (B and E) Ratios of EPSC decay times at high- and low- P_r conditions demonstrate that, while all values are clustered around unity for the uEPSCs, three-quarters of the evoked responses had values $>$ 1.25. (C and F) Postsynaptic EPSCs from the beginning (light grey) and end (black) of stimulus train from representative cells (C, AB537; F, AB528). Insets show the amplitude-normalized traces with superimposed exponential fits. The upper traces indicate the type of stimuli: (C) action potential and (F) square current pulse. Scale bars, 2 ms (1.4 ms for inset); 52 mV and 10 pA (C); 2 ms (1.8 ms for inset); 50 pA (F).

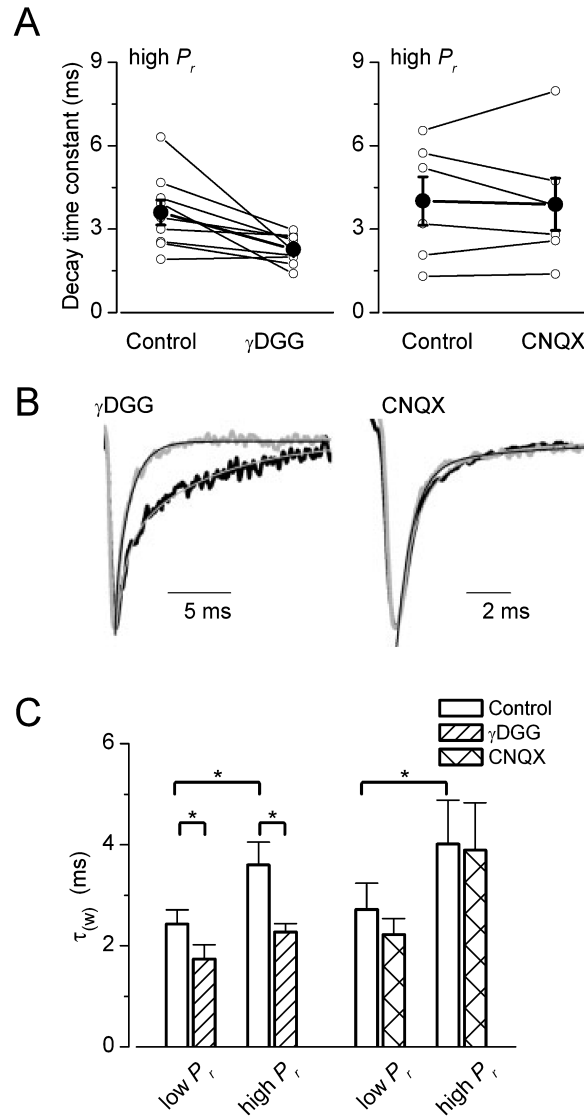


Fig. 3. Differential effects of a low- and a high-affinity glutamate receptor antagonist on the decay of evoked EPSCs. (A) γ DGG speeds up the decay time constant (τ) of eEPSCs at high release probability conditions by $\approx 37\%$ (panel) ($n = 9$). In contrast to γ DGG, the high-affinity antagonist CNQX (right) does not change significantly the decay of EPSCs at the end of the stimulus train (O, individual cells; •, mean \pm SEM). (B) Amplitude-normalized averaged traces at the end of stimulus trains in control (black) and in drugs (light grey). Thin lines are the exponential fits to the decaying phase of EPSCs. γ DGG speeded up (from 3.9 to 1.4 ms in AB521), whereas CNQX did not alter the decay time constants (from 1.3 to 1.4 ms in AB498). (C) Summary of drug effects on eEPSC decay times at low- and high- P_r conditions. Mean values + SEM are shown. The decay of eEPSCs increased significantly from the beginning to the end of the trains in the control period of γ DGG ($n = 9$) and CNQX ($n = 6$) application. γ DGG reduced significantly the τ of eEPSCs both at the beginning and end of the trains ($P < 0.05$, t -test), while CNQX did not have any effect on decay kinetics of EPSCs.